ote technical note tech

Determining the Equivalent Thermal Gradient for Rigid Pavements at the National Airport Pavement Test Facility

Daniel I. Offenbacker and David R. Brill

July 2024

DOT/FAA/TC-TN24/18

U.S. Department of Transportation

Federal Aviation Administration

Technical Report Documentation Page

1. Report No.	2. Government Accession No.	3. Recipient's Catalog No.
DOT/FAA/TC-TN24/18		

4. Title and Subtitle	5. Report Date
DETERMINING THE EQUIVALENT THERMAL GRADIENT FOR RIGID PAVEMENTS AT THE NATIONAL AIRPORT PAVEMENT TEST FACILITY	July 2024
	6. Performing Organization Code
7. Author(s)	8. Performing Organization Report No.
Daniel I. Offenbacker and David R. Brill	
9. Performing Organization Name and Address	10. Work Unit No. (TRAIS)
Federal Aviation Administration Aviation Research Division Airport R&D Technology Branch William J. Hughes Technology Center Atlantic City International Airport Egg Harbor Township, NJ 08405	
	11. Contract or Grant No.
12. Sponsoring Agency Name and Address	13. Type of Report and Period Covered
U.S. Department of Transportation Federal Aviation Administration Airport Engineering Division 800 Independence Ave., SW Washington, DC 20591	Technical Note
	14. Sponsoring Agency Code AAS-110

15. Supplementary Notes

16. Abstract

In recent years, the Federal Aviation Administration (FAA) has focused on identifying and quantifying corner breaking in rigid airport pavements. Prior research studies at the FAA National Airport Pavement Test Facility (NAPTF) have shown premature corner breaks that were not anticipated during design. The FAA has since attributed the corner breaks to Portland Cement Concrete (PCC) curling occurring in the NAPTF; however, little research effort has been aimed at quantifying the severity of PCC curling. Thus, the purpose of this research study was to quantify the severity of PCC curling occurring at the NAPTF using information and data Construction Cycle 1, Construction Cycle 2, and Construction Cycle 6. The research study quantified PCC curling through an Equivalent Thermal Gradient (ETG), which included temperature, shrinkage, and permanent (built-in) gradients. The ETG was calculated using literature, environmental, and thermocouple data collected from within the PCC slabs. In parallel, ETGs were backcalculated using finite element analysis and instrumentation data collected during each NAPTF construction cycle. The finite element analysis included thermal and aircraft loading similar to the conditions of the respective experiment. Finally, the calculated and backcalculated ETGs were then compared to determine an appropriate ETG for the NAPTF. Based on the findings from this research study, the rigid pavements at the NAPTF experience an ETG range of approximately -3.0 to -6.0 °F/inch. Further, the primary cause of curling at the NAPTF was found to be associated with permanent curling experienced during construction.

17. Key Words	18. Distribution Statement
Airport pavement design, Portland Cement Concrete, Curling, Equivalent Thermal Gradient	This document is available to the U.S. public through the National Technical Information Service (NTIS), Springfield, Virginia 22161. This document is also available from the Federal Aviation Administration William J. Hughes Technical Center at actlibrary.tc.faa.gov.

19. Security Classif. (of this report)	20. Security Classif. (of this page)	21. No. of Pages	22. Price
Unclassified	Unclassified	31	

TABLE OF CONTENTS

LIST OF FIGURES

LIST OF TABLES

LIST OF ACRONYMS

2D	Dual tandem
3D	Dual tridem
CBR	California bearing ratio
CC	Construction Cycle
ETG	Equivalent thermal gradient
FAA	Federal Aviation Administration
FEAFAA	Finite Element Analysis for Federal Aviation Administration
HWD	Heavy-weight deflectometer
ML	Machine learning
NAPTF	National Airport Pavement Test Facility
PCC	Portland Cement Concrete
SCI	Structural Condition Index

EXECUTIVE SUMMARY

Since 1999, the Federal Aviation Administration (FAA) has conducted full-scale traffic tests on rigid airport pavements at the National Airport Pavement Test Facility (NAPTF). At the first full-scale traffic test, the FAA experienced extensive corner breaks among all the rigid pavement slabs. The FAA determined that the rigid pavement slabs experienced curling, which led to the onset of corner breaks at the start of trafficking. In subsequent experiments, additional measures were taken to prevent curling from affecting the traffic tests. These measures included periodic watering, additional care and oversight during curing, and inclusion of fly ash. These measures were successful in mitigating corner breaks but did not completely prevent their occurrence. Thus, based on the recurring observation of corner breaks, better understanding of the rigid pavement curling at the NAPTF was needed.

The main purpose of this study was to utilize historical data from previous full-scale traffic tests and more modern tools (such as Finite Element Analysis) to better understand rigid pavement curling at the NAPTF. The study included data from three separate experiments—Construction Cycle 1, Construction Cycle 2, and Construction Cycle 6—which were all rigid pavement experiments that experienced corner breaks. Climatic data inside the NAPTF, such as Relative Humidity and temperature, was also collected. Curling was quantified through the use of a universal measure called the Equivalent Thermal Gradient (ETG), which combines the effects of temperature, drying, and factors that yield a permanent curl. The ETG for each Construction Cycle was determined through two different methods: (i) empirical estimation and (ii) Finite Element Analysis backcalculation.

The results of this study showed that the ETG ranged between -2.3°F/inch and -5.9°F/inch depending on the experiment. Construction Cycle 1, which experienced the greatest number of corner breaks, had an estimated ETG between -4.5°F/inch and -5.5°F/inch and was more severe than the other experiments considered in this study. Further, permanent curling (including curling induced during construction) had the greatest contribution to the ETG levels specifically due to the time of the year these pavements were constructed.

INTRODUCTION

BACKGROUND

The Federal Aviation Administration (FAA) is tasked with developing guidance and specifications for the design and construction of commercial airport pavements. In this effort, the FAA owns and operates the National Airport Pavement Test Facility (NAPTF), which is a full-scale indoor airport pavement test facility designed to conduct accelerated testing on rigid and flexible pavements using traditional aircraft loads. Although the facility is protected from sun, wind, and precipitation, the NAPTF is not temperature or humidity-controlled, resulting in its own environmental state and impacting pavement behavior. One recurring pavement behavior associated with the NAPTF environment has been curling in Portland Cement Concrete (PCC) slabs. Specifically, curling (and resulting top-down corner breaks) has been observed in Construction Cycles 1, 2, and 6.

The purpose of Construction Cycle 1 (CC1) was to assess the impacts of subgrade strength and PCC slab thickness on bottom-up cracking in rigid pavements. Following design and construction, aircraft loading (both dual-tandem [2D] and dual-tridem [3D]) was applied to the CC1 rigid pavements. After the first day of trafficking, a majority of the CC1 rigid pavements experienced sudden corner breaks and were deemed failed. The short lifespan of the CC1 rigid pavements was unexpected and found to be from excessive curling in the CC1 rigid pavements. The outcomes from CC1 have since been documented in literature (General Dynamics Information Technology, 2019).

Subsequently, Construction Cycle 2 (CC2) was split into separate phases, the first of which was designated to investigate and quantify PCC curling. In CC2 Phase II, *Single Slab Experiment*, the FAA instrumented a single PCC slab with vertical displacement transducers on each corner of the slab and recorded the level of PCC curling for approximately 6 months after the PCC was placed. The FAA then evaluated the sensor data, identifying the greatest amount of curling in October 2003 and the lowest amount of curling in December 2003. The data from CC2 Phase II were then fit to five existing thermo-mechanical models that could estimate slab corner displacement using an Equivalent Thermal Gradient (ETG). Researchers concluded from CC2 that the ETG was higher than expected and that the modeling procedure needed to be refined further before any greater conclusions could be made (Guo et al. 2004). No further research was done to compare this ETG with CC1 data or to incorporate into future Construction Cycle experiments but, given the observed PCC curling behavior from CC2 Phase II, FAA took several precautions in an attempt to limit PCC curling in future NAPTF experiments and prevent premature corner breaks from occurring.

Even with these precautions, 13% of all slabs in CC2 Phase IV, *Main Experiment*, experienced corner breaks as the initial distress (Brill et al., 2005). For Construction Cycle 6 (CC6), corner breaks were observed in 63% of all slabs as the initial distress (Brill & Kawa, 2014). Thus, the FAA identified a need to better quantify the temperature and stress distribution in rigid pavements. Specifically, the top-down stresses were of interest to better relate the mechanistic responses to the flexural strength properties of the PCC.

FAA research into top-down stresses focused on (i) identification of various factors impacting top-down cracking and (ii) developing a machine learning (ML) model to quantify tensile stress along PCC surface (Ashtiani et al., 2022). Several interesting outcomes from these research studies were found, including:

- Slab dimensions impacted the top-down stress magnitude
- Critical top-down stress location was not found underneath an aircraft tire
- Critical offset (distance from longitudinal and transverse joint) of the aircraft gear was dependent on gear configuration
- Critical edge (longitudinal or transverse) varied based on joint spacing, joint stiffness, gear configuration, and additional factors

The current state of research provided insight into how aircraft configuration, pavement geometry, and rigid pavement joint conditions impacted the PCC top surface stresses (Ashtiani et al., 2022). The FAA research on top-down cracking also considered ETG using parametric analysis to obtain a general range of top-down stresses. However, no research was aimed at determining an appropriate temperature distribution for the NAPTF. Therefore, it is necessary to establish a method for computing ETG for concrete test pavement at the NAPTF. Calculating ETG for the NAPTF concrete test pavements can lead to better interpretation of corner break data collected from CC1, CC2, and CC6 and, ultimately, be used to develop a top-down PCC cracking failure model.

RESEARCH GOAL AND OBJECTIVES

The goal of this study was to quantify the stresses from PCC curling and aircraft loading from CC1 and CC6 and compare them with the recorded pavement performance data. The NAPTF was selected for this study because of its extensive instrumentation data and repeated experiments (CC1, CC2, and CC6) that allow for multiple datapoints. The objectives of this research study were to:

- Review design, construction, instrumentation, and trafficking plans from CC1, CC2, and CC6
- Estimate ETG using collected temperature and relative humidity data in NAPTF
- Simulate CC1 and CC6 aircraft loading using the FAA's three-dimensional Finite Element Analysis (FEAFAA) with a variable range of ETG
- Identify the ETG that provides a similar mechanistic response to the respective Construction Cycle data

REVIEW OF PREVIOUS NAPTF RIGID PAVEMENT CONSTRUCTION CYCLES

CONSTRUCTION CYCLE 1

DESIGN AND CONSTRUCTION. CC1 included rigid pavements that varied in subgrade strength and PCC slab thickness. The PCC slabs were built 20 feet by 20 feet with 25-foot transition sections separating rigid pavement test sections. Longitudinal joints were built as construction joints and transverse joints were built as contraction joints. All longitudinal joints were doweled, but transverse joints were undoweled. Subgrade strengths were measured using the California Bearing Ratio (CBR) test, and values varied by test section between 3 and 30. The same PCC mixture was used throughout all slabs with a target flexural strength of 740 psi. As part of the experiment, PCC slab thickness varied between 9 and 11 inches depending on the respective pavement subgrade. Figure 1 provides general information and representation of the various rigid pavements included in CC1.

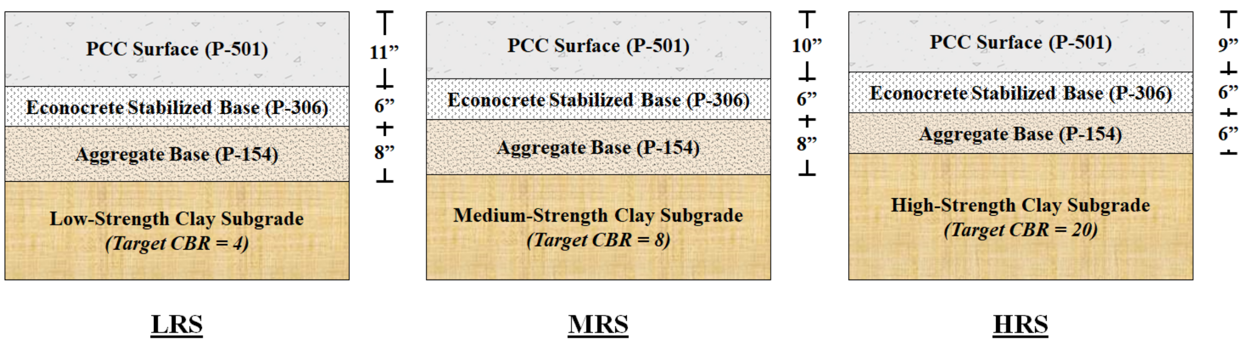

Figure 1. Cross-Sectional Views of Construction Cycle 1 Rigid Test Items

TRAFFICKING. Aircraft trafficking began on February 14, 2000, using a wheel load of 45,000 pounds and tire pressure of 188 psi. Depending on the test section location, aircraft gear configurations in the North and South test sections were 3D and 2D, respectively. Aircraft loading was wandered laterally using a set wander pattern of 9 distinct vehicle tracks spread across 66 passes.

FINDINGS. Unexpectedly, most rigid pavement sections in CC1 experienced a corner break within the first day of trafficking. Upon continuation of trafficking, corner breaks were eventually observed on all CC1 rigid pavement slabs. It was observed that the high- and medium-strength subgrade areas experienced corner breaks before the low-strength subgrade area. Further research found that the high-strength subgrade slabs experienced the greatest amount of curling and the low-strength subgrade slabs experienced the least amount of curling. Confirmation of this trend in PCC curling was done through Heavy Weight Deflectometer (HWD) testing and deflection measurements. Additional information pertaining to CC1 can be found in its respective comprehensive report (General Dynamics Information Technology, 2019).

CONSTRUCTION CYCLE 2 PHASE II—SINGLE SLAB EXPERIMENT

DESIGN AND CONSTRUCTION. CC2 Phase II was designed, in response to CC1, to solely evaluate PCC curling within the NAPTF without the influence of aircraft loading. A single 15-

foot-by-15-foot PCC slab was built in June 2003 with slab thickness of 11 inches. The PCC slab was placed on top a of 20-foot-by-20-foot PCC slab with a bond breaker in between each PCC layer. The edges of the slab were left unconstrained to allow for free movement and curling. The PCC slab was wet cured for 28 days using burlap strips, soaker hoses, and plastic sheet coverings. After a 28-day wet curing, all coverings were removed, and the slab was allowed to dry. Vertical displacement, horizontal displacements, concrete strain gauges, thermocouples, and relative humidity sensors were installed. Sensor measurements were taken for a span of 113 days. Slab dimensions and instrumentation are presented in Figure 2.

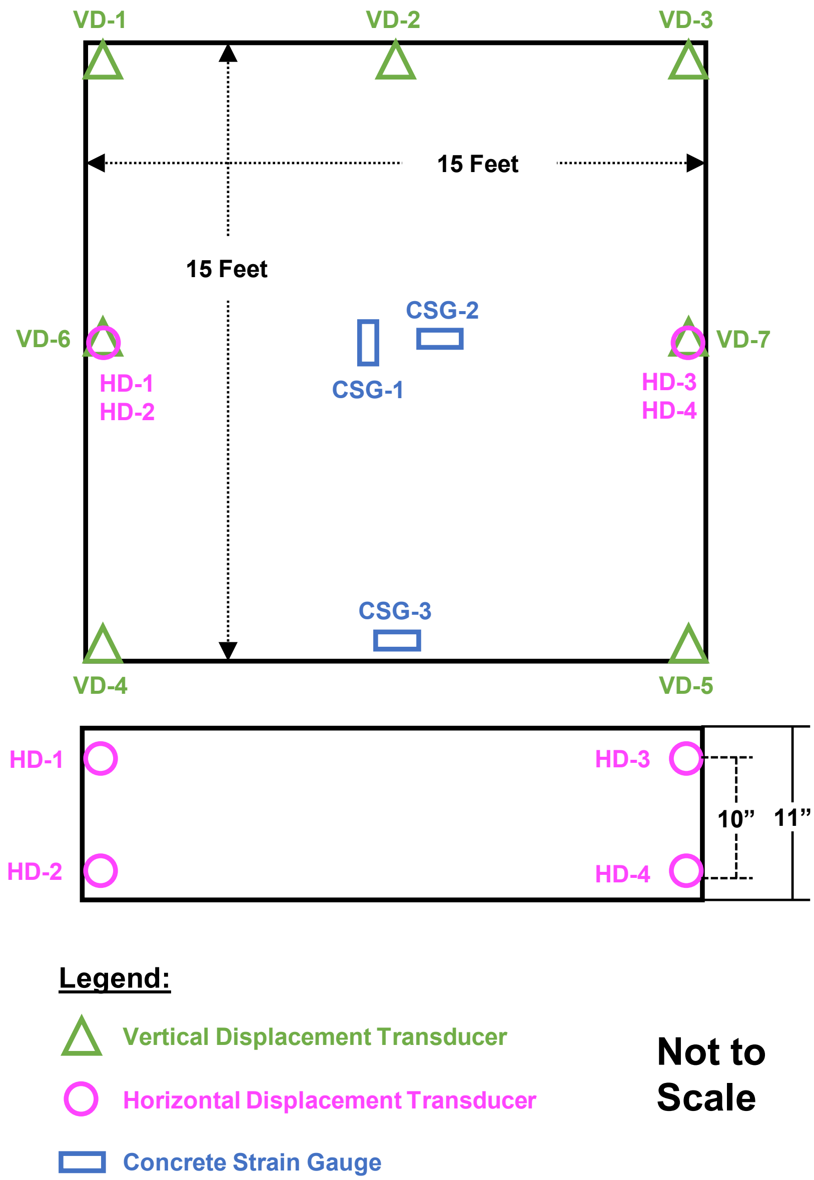

Figure 2. Slab Dimensions and Instrumentation Layout for CC2 Phase II—Single Slab Test Item

FINDINGS. CC2 Phase II provided a unique dataset showing the curling behavior of P-501 PCC without the influence of aircraft loading. Based on vertical displacements measured at each corner of the slab, the most amount of curling was found to occur in October 2003 with peak displacements between 190 and 210 mils. The least amount of curling was observed in December 2003 with corner displacements between 54 and 74 mils. Corner displacements were always positive (corner moved upwards) throughout the duration of the experiment. The results from CC2 Phase II are presented in Figure 3 with annotations to denote the recorded PCC displacements. Based on the recorded measurements from CC2 Phase II, the ETG was determined to be between -4.8 °F/inch and -5.8 °F/inch (Guo et al., 2004).

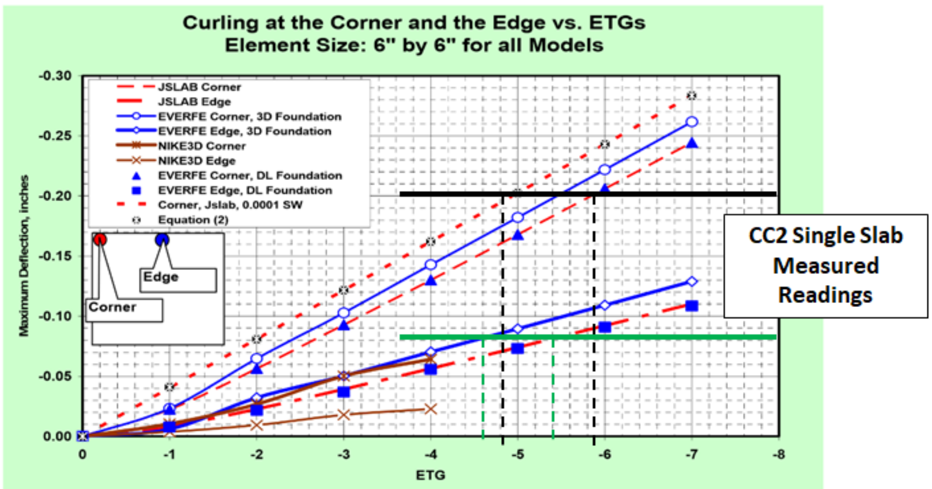

Figure 3. Curling Displacements Estimated in Single PCC Slab Annotated with Measured Readings CC2 Phase II (adapted from CC2 Phase II website)

CONSTRUCTION CYCLE 6

DESIGN AND CONSTRUCTION. CC6 was designed to solely investigate the performance of rigid pavements. CC6 consisted of 76 slabs (15 feet long by 15 feet wide) and were doweled in the longitudinal and transverse directions. Smaller slab dimensions and additional load transfer were included in the CC6 experimental plan to minimize the risk of slab curling. Variables included in the CC6 experiment were different stabilized bases—Hot Mix Asphalt in North test sections and Econocrete in South test sections—and flexural strength of the PCC. Specifically, the 28-day flexural strength was 662; 763; and 1,007 psi depending on the test section. Cross-sectional views of the CC6 test sections are presented in Figure 4. CC6 in its entirety consisted of 203 sensors including 174 embedded concrete strain gauges. Each embedded strain gauge was installed as a pair with gauges embedded at 1.5 inches and 10.5 inches.

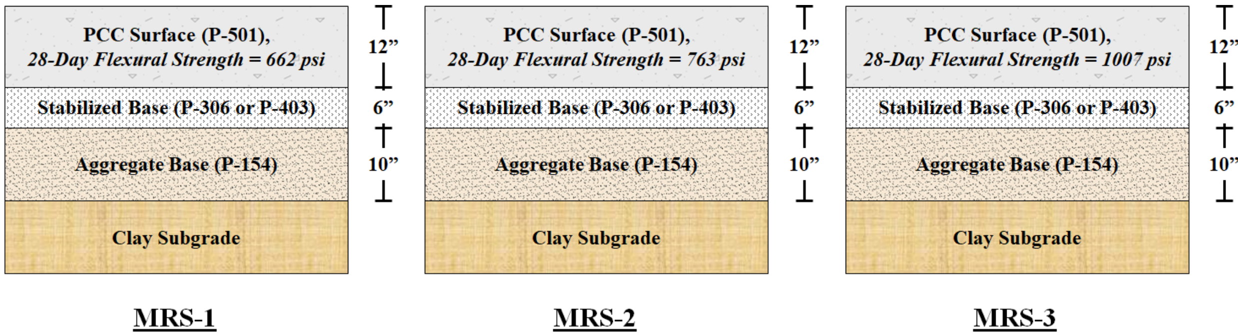

Figure 4. Cross-Sectional Views of CC6 Rigid Test Items

TRAFFICKING. Aircraft trafficking began in August 2011 and continued through April 2012. The wheel loads increased over the duration of the test with distinct wheel loads of 45,000; 52,000; and 70,000 pounds. 2D gear configuration was used on all sections and tire pressure was kept constant at 188 psi. Aircraft loading was wandered laterally using a set wander pattern of nine distinct vehicle tracks spread across 66 passes.

FINDINGS. Outcomes from CC6 showed that the 28-day flexural strength was strongly correlated to the observed visual performance. In total, 64 of the 76 slabs experienced some form of distress, 49 of which were corner breaks (i.e., 77% of all slabs that had experienced distress had corner breaks). Further, the type of stabilized base (Econocrete or Hot Mix Asphalt) did not impact the overall Structural Condition Index (SCI), but a different crack pattern was observed between some sections (Brill & Kawa, 2014). The SCI results were then later used to refine the FAA rigid pavement design model (Brill & Kawa, 2014).

ESTIMATION OF EQUIVALENT THERMAL GRADIENT AT THE NAPTF

Curling is a phenomenon in PCC pavements where the slab experiences an upward or downward distortion causing a portion of the slab to become unsupported. Figure 5 presents an illustration of PCC curling. Curling in PCC has been attributed to several factors including temperature changes, moisture changes (humidity and groundwater), trapped heat during construction, PCC mix properties, and creep effects.

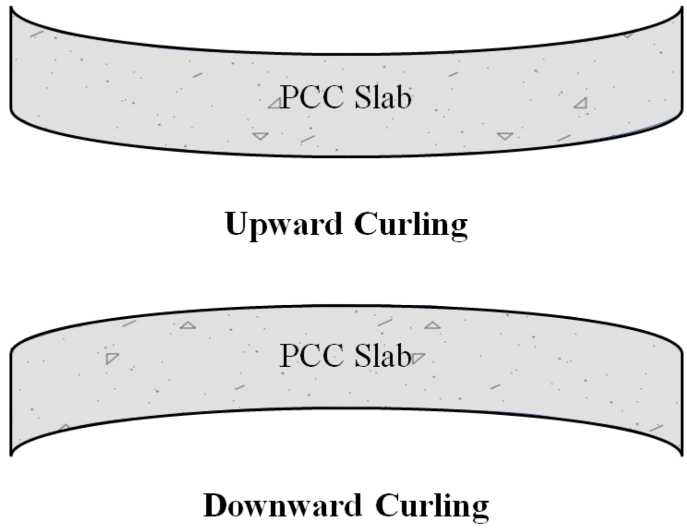

Figure 5. Illustration of Upward and Downward Curling in PCC Slabs

Due to the simultaneous and combined behavior of the PCC curling factors, an ETG is typically used to model PCC curling (Guo, 2001; Brill et al., 2005). ETG converts all causes of PCC curling into a single temperature differential (throughout the PCC slab thickness). This temperature differential measure has been defined as the total equivalent temperature differential and is the summation of all causes of PCC curling as shown in Equation 1 (AASHTO, 2015).

$$\Delta T_{Total} = \Delta T_{Temperature} + \Delta T_{Shrinkage} + \Delta T_{Built-In} \quad (1)$$

Where:

ΔT_{Total} = Total equivalent temperature differential, °F
$\Delta T_{Temperature}$ = Temperature differential in PCC slab from top surface to bottom surface, °F
$\Delta T_{Shrinkage}$ = Equivalent temperature differential due to PCC moisture changes, °F
$\Delta T_{Built\text{-}In}$ = Equivalent temperature differential built in during construction, °F

Each factor in Equation 1 is calculated separately using a variety of different techniques and methods depending on temperature, humidity, and seasonal factors during construction. Subsequent sections provide a description of how each factor was calculated in this study.

EQUIVALENT TEMPERATURE DIFFERENTIAL

The temperature differential in the slab has been the most widely researched and several efforts have been made to estimate the temperature differential using ambient temperature information along with PCC slab thickness (Zhao et al., 2020). In the case of this research study, the FAA installed thermocouples in the upper and lower portions of selected PCC slabs during each NAPTF experiment. Using this thermocouple data, the temperature differential was calculated as shown in Equation 2. Figure 6 presents the temperature differentials recorded during CC1, CC2, and CC6. It is noted that in CC1 only one test area was instrumented with thermocouples.

$$\Delta T_{Temperature} = \frac{\Delta T_{Top,i} - \Delta T_{Bottom,i}}{D} \times h \qquad (2)$$

Where:

$\Delta T_{Temperature}$ = Temperature differential in PCC slab from top surface to bottom surface, °F
$\Delta T_{Top,i}$ = Thermocouple reading during hour i at the top of PCC, °F
$\Delta T_{Bottom,i}$ = Thermocouple reading during hour i at the bottom of PCC, °F
D = Distance between top and bottom thermocouples, inches
h = Thickness of PCC slab, inches

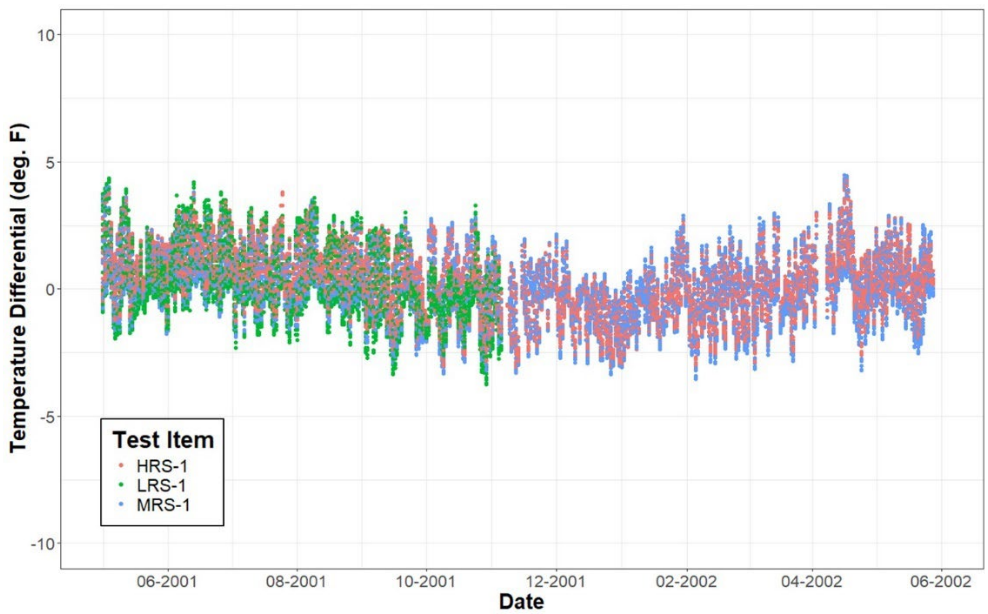

(a)

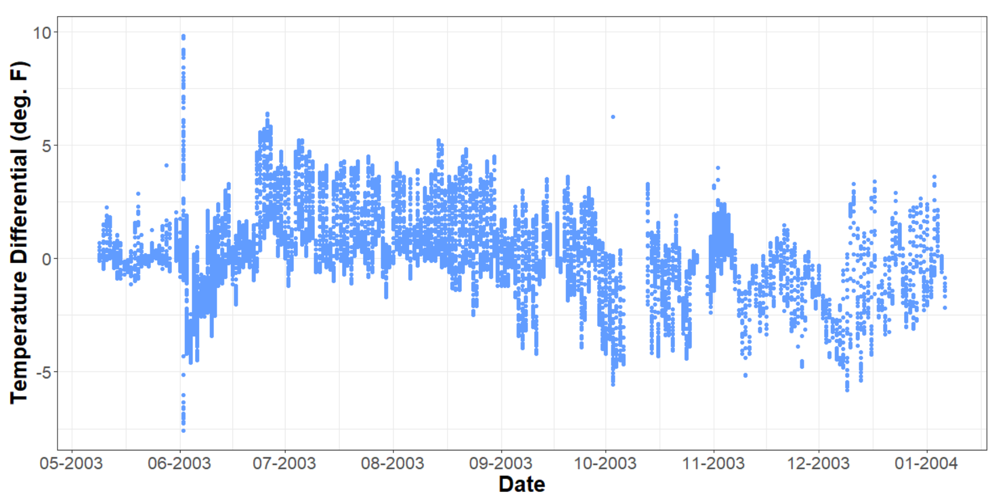

(b)

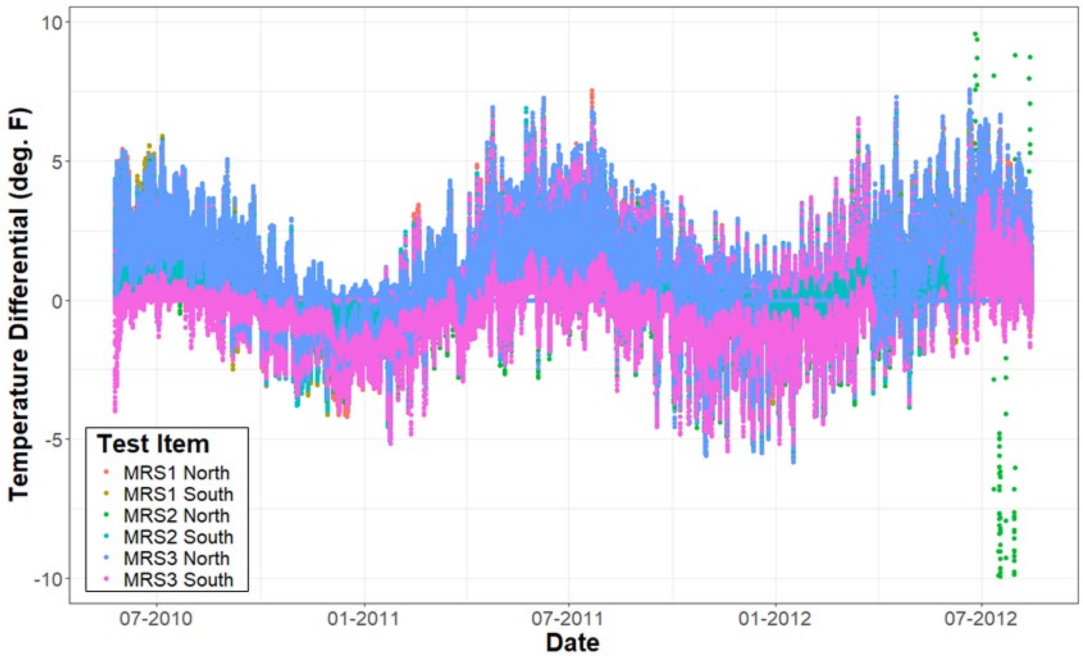

(c)

Figure 6. Temperature Readings from Thermocouples Installed within a PCC Slab Located at the NAPTF for (a) CC1, (b) CC2, and (c) CC6

As shown in Figure 6, the temperature differentials varied throughout the year and depending on the NAPTF experiment. This was expected given that there were different environmental, construction, and design conditions in each experiment. Additionally, there were some sporadic jumps (or drops) in temperature differential such as those observed in Figure 6c, MRS2 North. These sporadic changes in thermocouples are assumed to be due to defects in the sensor rather than physical measurements. Therefore, for further analysis in this study, the 99th percentile of data was used to determine ETG rather than the absolute minimum.

In addition to the temperature differentials from CC1, CC2, and CC6, the NAPTF installed thermocouples at both the upper and lower surfaces of a 12-inch PCC slab in 2016 as part of CC8 to take physical measurements of the temperature differential throughout the PCC slab. The readings were taken hourly for a span of almost 2 years between 2018 and 2020. These data, though not used directly within this study, were analyzed for future use in the case that thermocouple data are unavailable. Table 1 presents the monthly temperature differentials calculated from the PCC thermocouples using Equation 2. As can be seen from Table 1, the late fall and winter-early spring months experience a negative temperature differential (upward curling), whereas the summer months experience a positive temperature differential (downward curling). It is noted that the temperature differentials are presented on a monthly average basis, however, in this study, the hourly temperature differentials were determined and used to calculate the ETG. For example, in December 2018 the average temperature differential was -0.6 °F, whereas the critical hourly temperature differential (minimum, in this case) was -3.6 °F.

Table 1. Monthly Temperature Differential for PCC Slabs at the NAPTF

Year	Month	PCC Temperature Differential (°F)		Hourly PCC Temperature Differential (°F)		Critical Negative Thermal Gradient (°F/inch)
		Mean	St. Dev	95% Min.	95% Max.	
2018	12	-0.65	1.19	-2.65	1.12	-0.29
2019	1	-0.48	0.97	-2.32	1.12	-0.26
2019	2	-0.16	0.90	-1.61	1.59	-0.18
2019	3	-0.16	1.35	-2.25	2.15	-0.25
2019	4	0.98	1.31	-1.07	3.20	-0.12
2019	5	1.09	1.51	-1.25	3.65	-0.14
2019	6	1.33	1.44	-0.94	3.73	-0.10
2019	7	1.44	1.37	-0.60	3.69	-0.07
2019	8	0.49	1.05	-1.36	2.18	-0.15
2019	9	0.19	1.22	-1.76	2.07	-0.20
2019	10	-0.41	1.19	-2.24	1.46	-0.25
2019	11	-1.36	1.33	-3.99	0.67	-0.44
2019	12	-0.85	1.36	-2.95	1.22	-0.33
2020	1	-0.62	1.19	-2.82	1.21	-0.31
2020	2	-0.34	1.19	-2.51	1.49	-0.28
2020	3	0.20	1.21	-1.78	2.38	-0.20
2020	4	0.12	0.98	-1.56	1.71	-0.17
2020	5	0.82	1.16	-1.10	2.81	-0.12
2020	6	1.33	1.11	-0.52	3.12	-0.06
2020	7	1.30	0.95	-0.07	2.93	-0.01
2020	8	0.45	1.02	-1.16	2.23	-0.13

EQUIVALENT TEMPERATURE DIFFERENTIAL DUE TO SHRINKAGE

Calculation of an equivalent temperature gradient due to PCC shrinkage is less intuitive as it requires measurement of soil moisture under PCC, humidity, and other sources of moisture and conversion of those to an equivalent temperature gradient. Several methods have been established for estimating an equivalent temperature differential due to PCC shrinkage (Tian, et al., 2023; Eisenmann & Leykauf, 1990). For this study, the method proposed by Lederle and Hiller (2012) was used to estimate $\Delta T_{Shrinkage}$ following Equation 3.

$$\Delta T_{Shrinkage} = \frac{\varphi Я \omega \varepsilon_{su} h_s[-3h(-4+\pi)-20h_s+6\pi h_s](1-\mu)}{2h^2\alpha} \tag{3}$$

$$Я = 1 - \left(\frac{RH}{100}\right)^2 \tag{4}$$

$$\omega = \begin{Bmatrix} 3.6308(^{w}/_{c}) - 0.5675, {}^{w}/_{c} \le 0.36 \\ 0.5463(^{w}/_{c}) + 0.4901, {}^{w}/_{c} > 0.36 \end{Bmatrix} \tag{5}$$

$$\varepsilon_{su} = C_1 C_2 (26w^{2.1} {f'}_c^{-0.28} + 270) \tag{6}$$

Where:

φ = Shrinkage factor, 0.5
RH = Relative humidity, %
w = Water content of PCC mixture, lb/ft^3
c = Cement content of PCC mixture, lb/ft^3
C_1 = Cement type factor (Tian, et al., 2023)
C_2 = Curing type factor (Tian, et al., 2023)
f'_c = 28-day PCC compressive strength, psi
h_s = Depth of shrinkage zone, 2.0 inches (Lederle R. , 2011)
μ = Poisson's ratio, 0.15
α = PCC coefficient of thermal expansion, 0.00005 /°F

Slab dimensions, cement type, curing method, and PCC mixture properties could be determined from information gathered during the respective Construction Cycle. Relative humidity within the NAPTF was measured alongside the instrumented PCC slab in CC8 and those data were used for Equation 4. All remaining factors needed for Equations 3–6 were assumed from literature. A summary of ETG from PCC shrinkage and the respective factors for CC1, CC2, and CC6 are presented in Table 2.

Table 2. Summary of Factors Used to Calculate the Equivalent Temperature Differential for PCC Drying Shrinkage at the NAPTF

Variable	**Unit**	**CC1**			**CC2**	**CC6**		
		LRS	MRS	HRS	Single Slab	MRS-1	MRS-2	MRS-3
w	lb/ft^3	7.9			9.25	12.0	8.5	8.7
c	lb/ft^3	17.4			18.5	17.0	18.5	25.2
C_1	-	1.0			1.0	1.0		
C_2	-	1.0			1.0	1.0		
f'_c	psi	3,708			3,590	3,020	4,178	6,427
h	inch	11	10	9	11	12		
RH^1	percent	39.5 to 97						
$\Delta T_{Shrinkage}^2$	°F	-6.5	-7.8	-9.7	-8.2	-14.5	-14.8	-13.3

<u>EQUIVALENT TEMPERATURE DIFFERENTIAL DUE TO BUILT-IN PCC GRADIENT</u>

Equivalent temperature differential associated with PCC thermal changes during construction are accounted for within $\Delta T_{Built\text{-}In}$. $\Delta T_{Built\text{-}In}$ is the most challenging equivalent temperature differential to calculate because (i) it only initiates after the PCC has experienced final set, but during the curing process, and (ii) it must disregard external temperature and moisture changes. At a specific point in time during PCC curing, no stresses exist within the PCC slab defined as the zero-stress time. The zero-stress time, and the amount of PCC curling experienced at the zero-stress time, is then used to determine $\Delta T_{Built\text{-}In}$. Several factors can impact the zero-stress time including environmental conditions during curing, construction practices and curing method, slab thickness, and PCC mixture properties. Because of the complexity in calculating the zero-stress time, research studies have been conducted in an effort to quantify appropriate zero-stress time and $\Delta T_{Built\text{-}In}$ values.

Nassiri (2011) completed a dissertation focusing on the calculation of built-in temperature gradients using instrumented PCC pavements in Philadelphia, Pennsylvania. The PCC pavements were instrumented with static strain gauges and thermocouples that were operating while the PCC was allowed to cure. The research study also included paving the rigid pavements at different times of the day to assess how the time affected the built-in temperature gradient. The data collected from this study, specifically, were pertinent given the considerably similar environmental conditions to the NAPTF (New Jersey) and the use of similar slab thicknesses as CC1, CC2, and CC6. The built-in temperature gradients reported by Nassiri (2011) for doweled and undoweled slabs in Philadelphia are presented in Table 3 and Table 4, respectively.

Table 3. Built-In Curl/Warp Temperature Gradient (°F/inch) for Doweled Rigid Pavements in Philadelphia, Pennsylvania (Nassiri, 2011)

Month of Construction	**Age of Pavement (Months)**						
	0	2	6	16	28	41	52
March	-1.0	-1.5	-3.0	-3.0	-3.0	-3.0	-3.0
April	-0.5	-1.0	-2.5	-2.5	-2.5	-2.5	-2.5
May	0.5	-0.5	-1.5	-1.5	-1.5	-1.5	-1.5
July	1.0	0.0	-1.5	-1.5	-1.5	-1.5	-1.5
September	0.5	0.5	-1.5	-1.5	-1.5	-1.5	-1.5
October	0.0	-0.5	-1.5	-1.5	-1.5	-1.5	-1.5
November	0.0	-1.0	-2.0	-2.0	-2.0	-2.0	-2.0

Table 4. Built-In Curl/Warp Temperature Gradient (°F/inch) for Undoweled Rigid Pavements in Philadelphia, Pennsylvania (Nassiri, 2011)

Month of Construction	**Age of Pavement (Months)**						
	0	2	6	16	28	41	52
March	-1.0	-2.0	-3.5	-3.5	-4.0	-4.0	-4.0
April	-0.5	-1.5	-3.0	-3.0	-3.5	-3.5	-3.5
May	0.5	-0.5	-2.0	-2.5	-2.5	-2.5	-2.5
July	1.0	-0.5	-2.0	-2.0	-2.5	-2.5	-2.5
September	0.5	-0.5	-2.0	-2.5	-2.5	-2.5	-2.5
October	0.0	-1.0	-2.0	-2.5	-2.5	-2.5	-2.5
November	0.0	-1.0	-2.5	-3.0	-3.0	-3.0	-3.0

Using information reported by Nassiri (2011), along with information gathered on the construction of CC1, CC2, and CC6, the equivalent temperature differential associated with the built-in PCC gradient could be estimated. Table 5 shows the date of PCC placement, reinforcement along joints, and age of pavement before trafficking. Based on the information reported in Table 6, the equivalent temperature differential was then calculated.

Table 5. Summary of Factors Used to Calculate the Built-In PCC Temperature Gradient at the NAPTF

Factor	CC1	CC2	CC6
Date of Construction	February–March 1999	June 2003	March–April 2010
Duration before Trafficking (Months)	~ 11 to 12 months	~ 6 months[1]	~ 4 to 5 months
Joint Reinforcement	• Longitudinal joints were doweled. • Transverse joints were undoweled.	Undoweled (No adjacent slabs)	Longitudinal and transverse joints were doweled.
Estimated Critical ETG due to Built-In PCC Gradient (Table 3 & Table 4)	-3.5 °F/inch	-2.0 °F/inch	-3.0 °F/inch

[1]CC2 did not experience any trafficking but was monitored for approximately 6 months.

CALCULATION OF TOTAL EQUIVALENT THERMAL GRADIENT

Total ETG for PCC pavements built during CC1 and CC6 can be calculated by combining the effects of temperature, shrinkage, and built-in stresses separately. The ETG for each individual NAPTF experiment can be calculated using Equation 7.

$$ETG = \frac{\Delta T_{Temperature} + \Delta T_{Shrinkage} + \Delta T_{Built-In}}{h} \tag{7}$$

Table 6 presents a summary of each ETG factor, as well as the total temperature differential and ETG for each PCC pavement. Based on Table 6, the ETGs for CC1, CC2, and CC6 were approximately -4.75, -3.5, and -4.5 °F/inch, respectively.

Table 6. Calculation of Equivalent Thermal Gradient Considering the Effects of Temperature, Shrinkage, and Built-In PCC Gradient

Variable	**Unit**	**CC1**			**CC2**	**CC6**		
		LRS	MRS	HRS	Single Slab	MRS-1	MRS-2	MRS-3
$\Delta T_{Temperature}$	°F	-3.6	-3.6	-3	-4.9	-2.6	-2.9	-3.4
$\Delta T_{Shrinkage}$	°F	-6.5	-7.8	-9.7	-9.9	-14.5	-14.8	-13.3
$\Delta T_{Permanent}$	°F	-38.5	-35	-31.5	-22	-36	-36	-36
ΔT_{Total}	°F	-48.6	-46.4	-44.2	-36.8	-53.1	-53.7	-52.7
h	inch	11	10	9	11	12	12	12
ETG_{Total}	°F/inch	-4.4	-4.6	-4.9	-3.4	-4.4	-4.5	-4.4

PERFORMANCE EVALUATION OF RIGID PAVEMENTS AT THE NAPTF CONSIDERING EQUIVALENT THERMAL GRADIENT

The calculation of ETG using environmental data relies on historical data and empirical correlations. Due to this, there is still an underlying need to confirm that the calculated ETG values are representative of rigid pavements at the NAPTF. The challenge is that ETG or temperature differentials from shrinkage and built-in stresses cannot be directly measured. Therefore, to evaluate the veracity of the calculated ETG, the rigid pavements from CC1, CC2, and CC6 were modeled using finite element analysis at varying levels of ETG. Using the responses from the finite element analysis and the collected data from each NAPTF experiment, a representative ETG could then be determined. Further description of the ETG evaluation using finite element analysis is provided in the following subsections.

BACKCALCULATION OF ETG USING CONSTRUCTION CYCLE DATA AND FEAFAA

Backcalculation of ETG has been done by the FAA in the past using analytical models for slab curling. As part of CC2, the FAA backcalculated the ETG using existing thermo-mechanical models and instrumentation data from PCC slab without aircraft loading. These models, however, were not applied to CC1 or CC6 because they were incapable of applying thermal and aircraft loading, simultaneously. Since then, the FAA developed the FEAFAA to simulate the combined behavior of PCC curling and aircraft loading. FEAFAA also allowed for the relaxation of several original assumptions used in CC2 and facilitated load-transfer across multiple slabs. Thus, backcalculation of ETG was completed using FEAFAA for CC1, CC2, and CC6 considering the thermal and aircraft loading conditions. Figure 7 presents a flowchart of the analysis procedure.

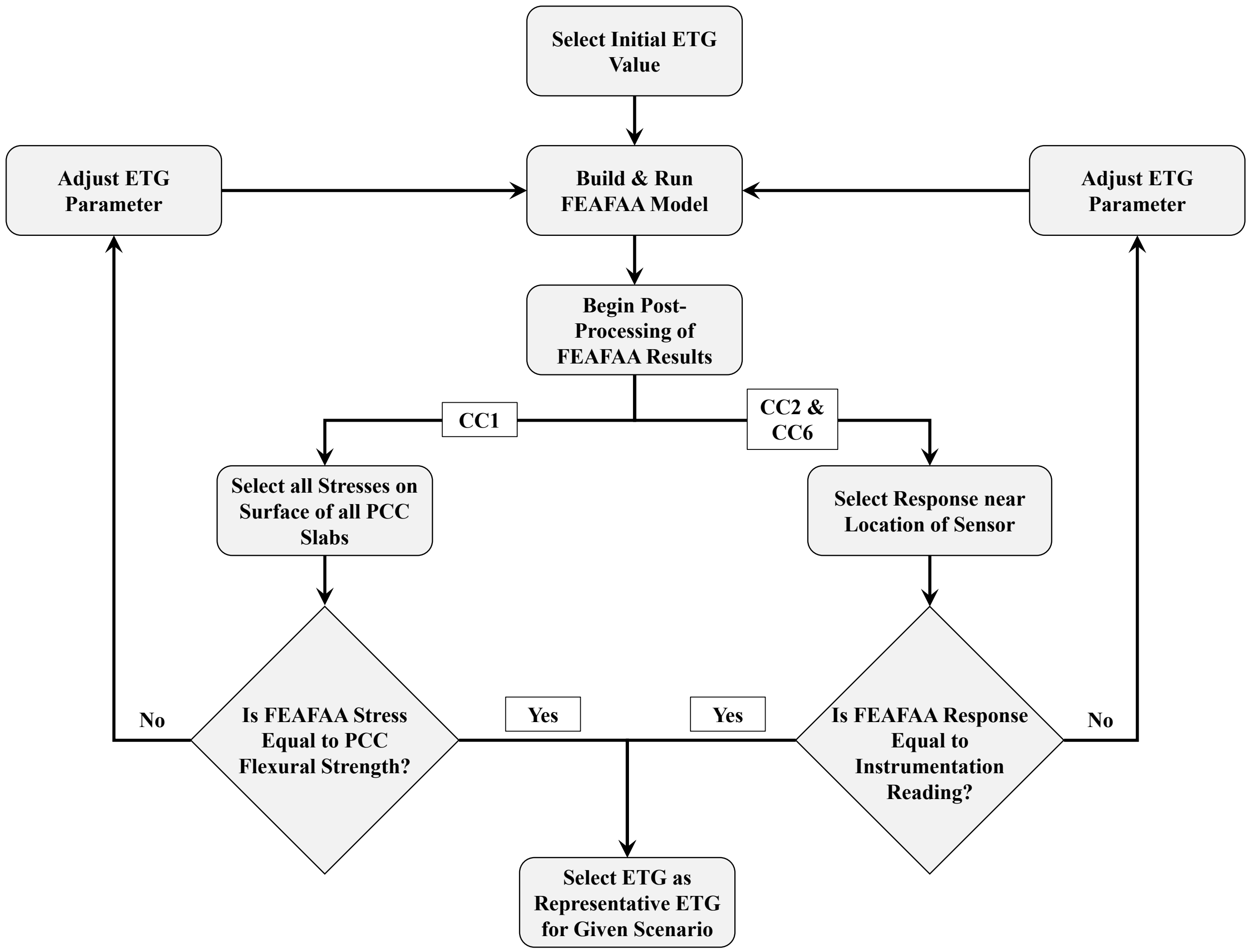

Figure 7. Equivalent Thermal Gradient Backcalculation Procedure using FEAFAA and Respective Construction Cycle Data

CC1 was a unique case because the pavements experienced top-down cracks within the first day of trafficking. Although the premature failure provided an interesting dataset for top-down cracking, it was unclear at what point sensors became biased by PCC cracking. Thus, direct comparisons between FEAFAA and instrumentation could not be made. However, understanding that the PCC failed almost immediately, it could be assumed that the top-down stresses experienced during CC1 were close to the flexural strength of the concrete. Therefore, direct comparisons were made between FEAFAA responses (and the ETG used as input) and the flexural strength of the PCC. For CC2 and CC6, the PCC slabs did not crack immediately and were instrumented with vertical displacement transducers (CC2) or strain gauges (CC6). So, for CC2 and CC6, direct comparisons were made between instrumentation readings during testing and the respective FEAFAA responses.

It is acknowledged that the ETG calculated from environmental and construction data (Table 6) was not expected to be directly equivalent to the backcalculated ETG from FEAFAA. The reason for this is because the reported flexural strength (or modulus of elasticity) is the average for the entire PCC mixture when, in fact, a corner break would occur at the weakest location. Further, once a corner break occurs, it will diminish the load transfer between slabs causing adjacent slabs to experience higher stress and crack faster. Thus, backcalculation of ETG using FEAFAA along with material properties or averaged sensor data was expected to have some error, but still considered reasonable for ETG estimation purposes.

DETERMINATION OF FEAFAA MODEL INPUT PARAMETERS

FEAFAA requires several different inputs relating to aircraft loading and gear configuration, pavement geometry and material properties, environmental conditions (i.e., ETG), joint conditions and the use of dowels, and location of aircraft gear with respect to the PCC joints. All FEAFAA inputs used in this study are presented in Table 7. Most inputs were assumed based on values from literature; however, in the case of CC1 and CC6, some FEAFAA inputs had to be determined from preliminary analyses (as noted in Table 7). CC2 did not require preliminary analysis for FEAFAA input parameters because it was a single slab experiment with no aircraft loading.

Table 7. FEAFAA Input Parameters Used During Preliminary Analysis to Determine Critical Stress Location and Gear Centroid Offset

FEAFAA Input Parameter	**CC1**
Aircraft Gear Configuration	3D
Wheel Load	45,000 lb
Offset from Longitudinal Joint (ft)	Unknown[1]
Offset from Transverse Joint (ft)	Unknown[2]
PCC Modulus (psi)	4,000,000
Stabilized Base Modulus (psi)	700,000
Number of PCC Slabs	9
Longitudinal Dowel Stiffness	210,000
Transverse Dowel Stiffness	10,000
ETG (°F/inch)	-4.0

For CC1, preliminary analysis was necessary to determine the critical offset from longitudinal joints. Based on literature, there was an additional need to determine critical stress direction (transverse or longitudinal) because CC1 used a 3D gear configuration (Ashtiani et al., 2022). In the CC1 preliminary FEAFAA analyses, 9 distinct vehicle tracks were used based on the testing summary documented in the CC1 final report (General Dynamics Information Technology, 2019). Figure 8 presents the maximum top surface stresses calculated by FEAFAA for both the longitudinal and transverse directions. Based on Figure 8, the transverse stress direction experienced the greatest tensile stress of 507.81 psi along Track +2. This critical track location corresponded to a gear centroid offset of 13 inches from the longitudinal joint.

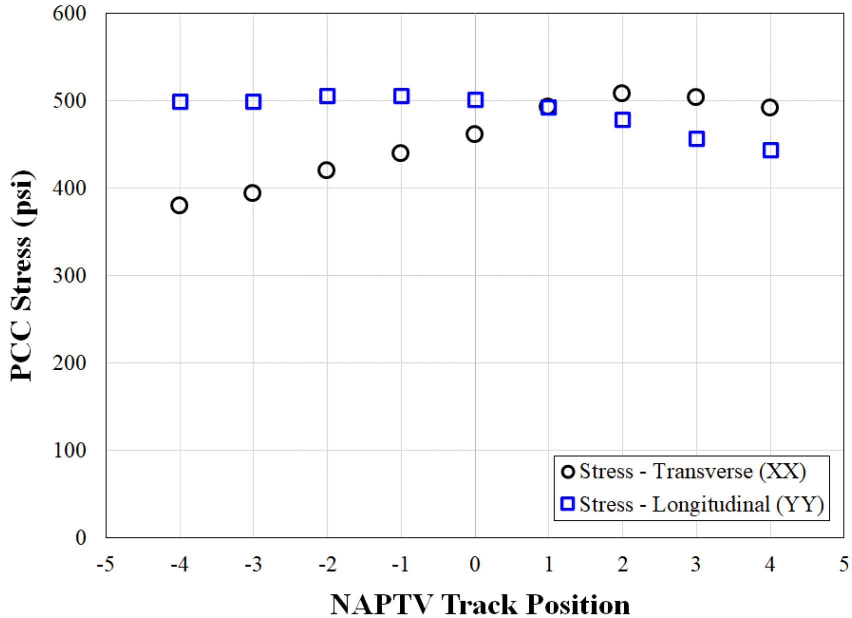

Figure 8. Top Surface Stresses Calculated by FEAFAA for Each Track in CC1

For CC6, the strain gauge responses were used directly rather than estimating the critical longitudinal joint using FEAFAA, where the greatest strain corresponds to the critical offset. Determination of critical stress direction was not needed to determine critical offset from the transverse joint due to the use of a 2D gear; however, both directions were still evaluated to simplify subsequent FEAFAA post-processing analyses. Figure 9 presents strain gauge readings from top of PCC for both the longitudinal and transverse directions.

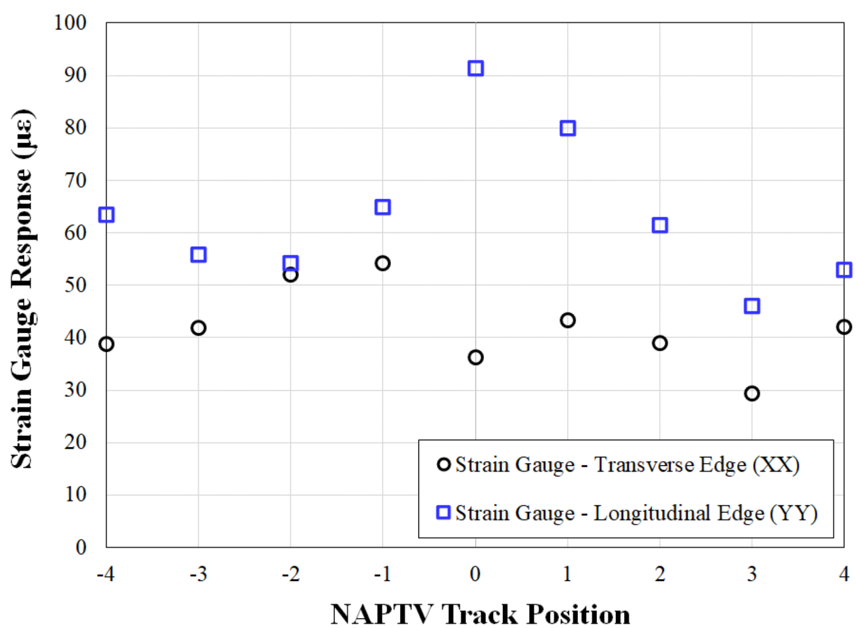

Figure 9. Portland Cement Concrete Strain Gauge Readings from Top Surface Strain Gauges for Each Track in CC6

As shown in Figure 3, in the case of CC6, the critical stress direction was along the longitudinal direction. Furthermore, the critical track appeared to be along Track 0, which corresponded to a gear centroid offset of 33 inches from the longitudinal joint. Based on the preliminary analyses presented in Figure 8 and Figure 9, all remaining FEAFAA inputs could be determined. Table 8 summarizes the final FEAFAA input parameters used in this study.

Table 8. Summary of Final FEAFAA Input Parameters Used to Model CC1 and CC6

FEAFAA Input Parameter	CC1	CC2	CC6
Aircraft Gear Configuration	3D	N/A	2D
Wheel Load	45,000 lb	N/A	45,000 lb
Offset from Longitudinal Joint (ft)	13 inches	N/A	33 inches
Critical PCC Edge Stress	Transverse	N/A	Longitudinal
Offset from Transverse Joint (ft)	-110.7 inches	N/A	-110.1 inches (ref)
PCC Modulus (psi)	4,000,000	4,000,000	4,000,000
Stabilized Base Modulus (psi)	700,000	700,000	700,000 (Econocrete) 400,000 (Asphalt)
Number of PCC Slabs	9	1	9
Longitudinal Dowel Stiffness	210,000	N/A	210,000
Transverse Dowel Stiffness	10,000	N/A	210,000
ETG (°F/in.)	-2 to -10	0 to -10	-1 to -6
Curling Shape	Spherical & Catenary	Catenary	Catenary

ANALYSIS OF RIGID AIRPORT PAVEMENTS AT NAPTF USING FEAFAA

Figure 10 and Figure 11 present FEAFAA analyses results using varying ETG levels for CC1 and CC2, respectively. For CC1, the curling shape—spherical and catenary—was also varied to evaluate the impact on estimated stress on the PCC surface. As shown in Figure 10, the FEAFAA-determined tensile stress approached the flexural strength of the PCC at an ETG of approximately -7.5 °F/inch and -5.5 °F/inch for spherical and catenary shapes, respectively. Comparing these FEAFAA-estimated ETG with ETG determined from environmental and construction data (Table 6), both measurements of ETG were considered similar when using a catenary curling shape. Significant differences in ETG were observed when using the spherical curling shape. As observed in Figure 11, ETG ranged between -5.9°F/inch and -2.3°F/inch depending on the time of year the corner displacements were taken. Interestingly, comparing CC1 and CC2 the extreme ETG measurements for catenary curling were similar in magnitude with values of -5.5 and -5.9°F/inch, respectively. Further, additional data is necessary to better understand yearly effects on the ETG value as those seen in Figure 11.

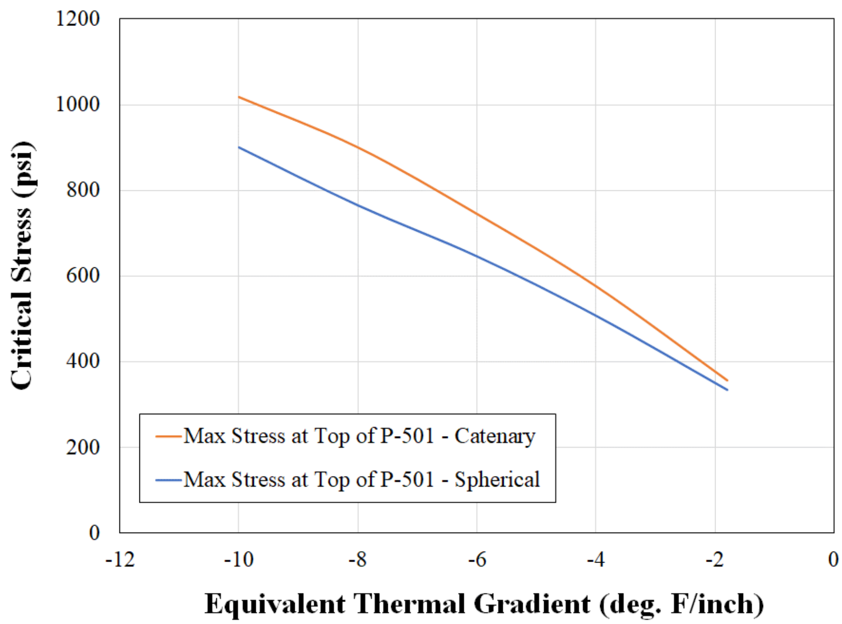

Figure 10. FEAFAA-Calculated Stress for Various ETG and Curling Shape in CC1

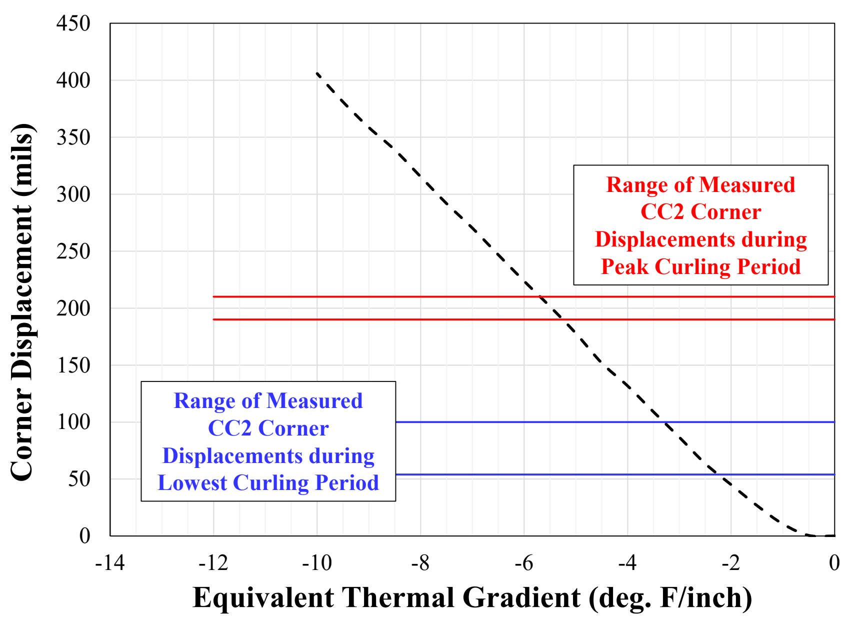

Figure 11. Construction Cycle 2-Measured and FEAFAA-Calculated Corner Displacements for Various ETG

Figure 12 presents FEAFAA analysis results using information from CC6. Additionally, the maximum and minimum strain gauge readings were converted to stress using the modulus assumed in FEAFAA (Table 8) and were presented in Figure 12 for comparison. As seen in Figure 12, the strain gauge readings intersected the FEAFAA results at an ETG between approximately -4.0 and -5.0 °F/inch. The top surface stresses were also significantly higher than the stress reported from the strain gauge due to the 1.5-inch embedment depth of the sensor. In comparison to CC1 (Figure 10), the top surface stress in CC6 did not approach the flexural strength of the concrete as seen in CC1. This corresponds with the longer pavement life observed in CC6 compared to CC1 and could be partially attributed to the added dowels along the transverse joint.

Using findings from CC1 and CC6 analyses, direct comparisons were made between the calculated ETG and backcalculated ETG from FEAFAA presented in Table 9. The calculated ETG and backcalculated ETG from CC2 were also included in Table 9 for comparison. Direct calculation of ETG was in general agreement with the ETG backcalculated using FEAFAA. Specifically, direct calculation of ETG was approximately 1.0 °F/inch greater than the backcalculated ETG for all CCs. The primary reason for this difference is assumed to be due to the critical condition assessment when determining the backcalculated ETG. In the case of the calculated ETG, average values for a specific time period are used to determine some factors (such as the relative humidity factor). The backcalculated ETG evaluates the most critical condition (i.e., critical track) at a specific moment in time. Thus, these differences are believed to be due to granularity differences in evaluation methods. Nonetheless, the direct calculation provides a sufficient measurement to estimate an appropriate ETG for rigid pavements.

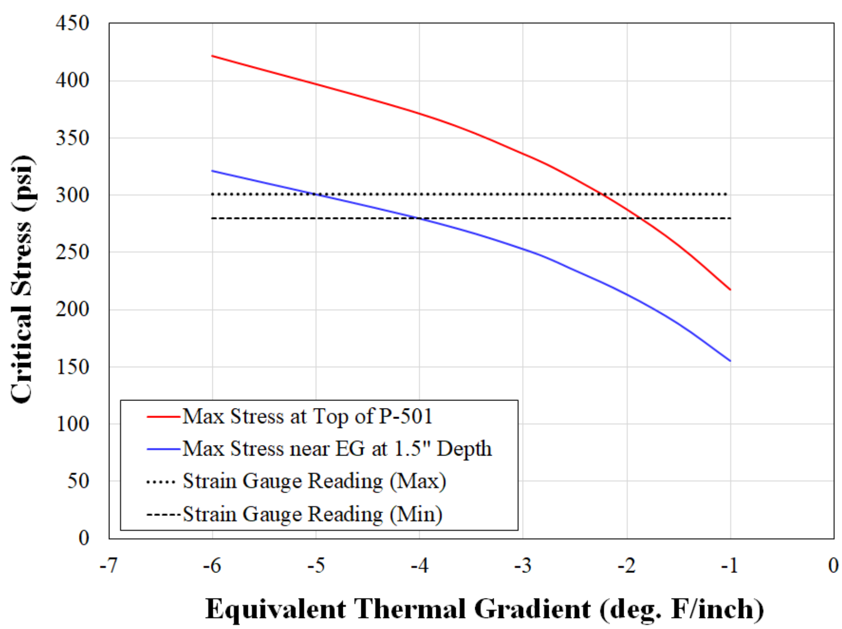

(a)

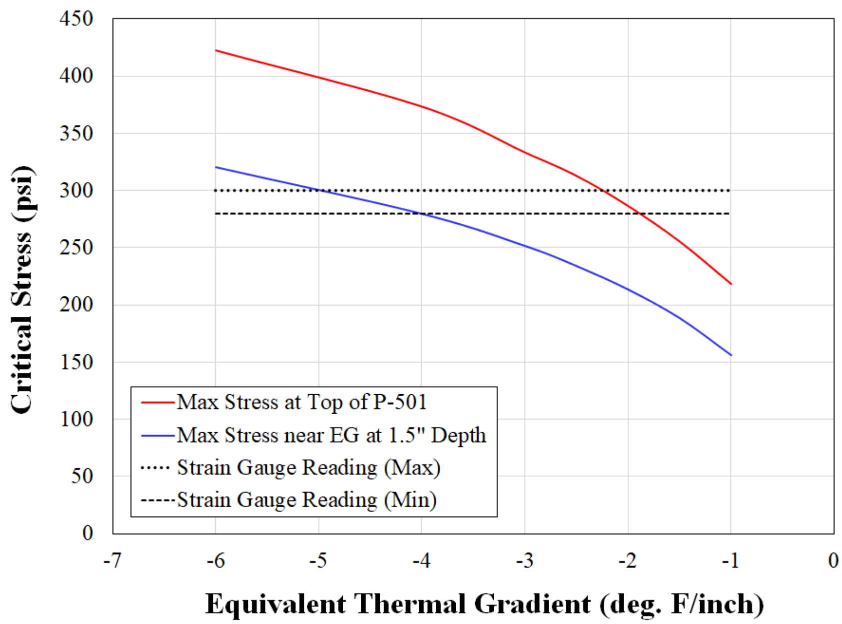

(b)

Figure 12. Finite Element Analysis for Federal Aviation Administration-Calculated Stress and Stress Estimated from Strain Gauge Readings for CC6 (a) Econocrete-Stabilized Base and (b) Hot Mix Asphalt-Stabilized Base

Table 9. Summary of ETG using Direct Calculation and FEAFAA Backcalculation Methods

ETG Measurement Method	ETG (°F/inch)		
	Direct Calculation	Backcalculation	
		Min	Max
CC1	-4.4 to -4.9	-5.5	
CC2	-3.4	-2.3 to -3.3	-5.2 to -5.9
CC6	-4.4 to -4.5	-4.0	-5.0

SUMMARY AND CONCLUSIONS

Prior research studies at the NAPTF identified corner breaks as a major distress for rigid airport pavements. The FAA attributed the corner breaks to substantial PCC curling but no direct relation between the severity of PCC curling (i.e., ETG) and rigid airport pavement performance had been studied. Thus, the purpose of this study was to quantify the ETG of rigid pavements at the NAPTF using historical data. As part of this study, the ETG at the NAPTF was directly calculated from environmental data along with relevant data from literature. In addition to the ETG calculation, FEAFAA analyses were completed at various ETG levels, and the mechanistic responses were compared to instrumentation data collected during each Construction Cycle. Using the two ETG estimation methods, an appropriate ETG for each NAPTF Construction Cycle could be estimated.

The conclusions from this study were:

- ETG of the NAPTF during CC1, CC2, and CC6 varied between -2.3 to -5.9 °F/inch depending on the Construction Cycle and ETG calculation method.

- Methodology used to calculate ETG from environmental data (and literature) provided a reasonable estimate of ETG compared to the backcalculated ETG. Generally, for CC1, CC2, and CC6 the ETG estimated from environmental data was approximately 0.5 °F/inch greater than the average backcalculated ETG.

- CC6 had lower reported ETG and PCC top surface stresses compared to CC1 with combined thermal and aircraft loading. Tensile stresses predicted for CC1 exceeded PCC flexural strength at the PCC surface due to severe ETG. Prevention of immediate corner breaks in CC6 can be partially attributed to the addition of dowels along the transverse joint.

- Curling shape used to model PCC curling had a substantial impact on the tensile stresses predicted in FEAFAA. Catenary curling shape (FEAFAA input parameter) provided PCC stresses that better agreed with CC1 findings compared to the spherical curling shape.

- Built-in temperature gradient served as the greatest contributor to ETG due to the date of construction.

REFERENCES

American Association of State Highway and Transportation Officials (AASHTO). (2015). *Mechanistic-Empirical Pavement Design Guide.*

Ashtiani, A., Paniagua, T., Parsons, T., & Foderaro, G. (2022). *Machine learning solutions for top-down cracking design of airport rigid pavement* (DOT/FAA/TC-22/44). Federal Aviation Administration.

Brill, D., & Kawa, I. (2014, August). *Relative performance of CC6 concrete pavement test items at the FAA National Airport Pavement Test Facility* [Paper] FAA Worldwide Airport Technology Transfer Conference, Galloway, New Jersey.

Brill, D., & Kawa, I. (2017). Advances in FAA pavement thickness design software: FAARFIELD 1.41. *Airfield and Highway Pavements 2017*, 92–102.

Brill, D., Hayhoe, G., & Ricalde, L. (2005, June). *Analysis of CC2 rigid pavement test data from the FAA's National Airport Pavement Test Facility* [Paper] Seventh International Conference on the Bearing Capacity of Roads, Railways and Airfields*,* Trondheim, Norway.

Eisenmann, J., & Leykauf, G. (1990, October). *Effect of paving temperature on pavement performance* [Paper]. 2nd International Workshop on Theoretical Design of Concrete Pavements, 419–428. Siguenza, Spain.

General Dynamics Information Technology. (2019, December). *National Airport Pavement Construction Cycle 1 (CC1) Comprehensive Report.* https://www.airporttech.tc.faa.gov/Portals/0/download/airport_pavement/CC1/Construction%20Cycle%201%20(CC1)%20Final%2012_02_2019.pdf?ver=2019-12-10-084238-370

Guo, E. (2001, September). *Back-estimation of slab curling and joint stiffness*, Paper presented at the Seventh International Conference on Concrete Pavements, Orlando, Florida.

Guo, E., Dong, M., Daiutolo, H., & Ricalde, L. (2004, January 1). *Analysis of the Observed and Predicted Responses of a Curled Single Slab* [Paper]. 2004 FAA Airport Technology Transfer Conference. https://www.airporttech.tc.faa.gov/Collaboration/Past-Conferences-Events/Airport-Technology-Transfer-Conference-2004/analysis-of-the-observed-and-predicted-responses-of-a-curled-single-slab

Lederle, R. (2011). *Accounting for warping and differential drying shrinkage mechanisms in the design of jointed plain concrete pavements* [Master's thesis, Michigan Technological University]. Digital Commons @ MTU. https://digitalcommons.mtu.edu/etds/251/

Lederle, R., & Hiller, J. (2012). New warping and differential drying shrinkage models for jointed plain concrete pavements derived with nonlinear shrinkage distribution, *Transportation Research Record, 2305*(1), 3–13.

Nassiri, S. (2011). *Establishing permanent curl/warp temperature gradient in jointed plain concrete pavements* [Doctoral dissertation, University of Pittsburgh].

Tian, K., King, D., Yang, B., Kim, S., Alhasan, A., & Ceylan, H. (2023). *Impact of curling and warping on concrete pavement: Phase II.* Iowa Highway Research Board.

Zhao, H., Li, C., Ma, L., Tian, Y., & Ling, J. (2020). Simple empirical temperature gradient prediction model for jointed plain concrete pavements: Development and validation. *Journal of Transportation Engineering, Part B: Pavements, 146*(3). https://doi.org/10.1061/JPEODX.0000190